Journal of Global Environment Engineering, Vol. 13, pp.69-96, 2008

NUMERICAL STUDY OF NO_x AND SO_x DYNAMICS UNDER LAND/SEA BREEZES IN DRY SEASON IN JAKARTA, INDONESIA

Asep Sofyan[1], Toshihiro Kitada[2], Gakuji Kurata[3]

Abstract

To investigate the effects of local flows on the distributions of NO_x and SO_x in Jakarta, numerical simulations were carried out for 6-17 August 2004 in dry season using a chemical transport model. The simulations well reproduced observed NO_2 and SO_2 fields, showing they were largely affected by land/sea breezes and mountain/valley winds; the pollutants discharged over Jakarta reached as far as 60 km inland, with the sea breeze and valley wind, in the late afternoon. Contrary, at night these moved 40-60 km off the coast with the mountain wind and land breeze enhanced by synoptic southeasterly. The dynamics of the pollutants' mass in the lower atmosphere over land and sea were examined; the SO_2 mass below 0.5 km high over Java Sea was large and 50~100% of that over the Jakarta area, indicating the land breeze combined with mountain wind was strong enough to result in large mass transport from land area to Java Sea during the nighttime. The sea breeze layer was limited to be shallow at 400~500m, and thus the pollutants discharged over Jakarta moved back and forth horizontally and accumulated in the shallow lower layer from day to day. Therefore, dry deposition process was important as removal mechanism of the pollutants, and the strength, the dry depositions of S- and N-compounds, was evaluated quantitatively, and compared with emissions.

KEYWORDS: *land and sea breeze, air pollution transport, Jakarta, NO_2, SO_2*

1. Introduction

Jakarta is located on the north coast of the western Java Island (see Fig. 1a). The area is 661.52 km^2 and its population is nearly 8.5 million; there are a large number of motor vehicles and industrial activities often causing serious air pollution problem. For example, Local Environmental Management Agency (BPLHD) of Jakarta city reported that in 2004 from 294 air-qualities monitored days, the Air Quality Index (AQI) levels of "good", "moderate", and "unhealthy" were 18 days (6.1%), 264 days (89.8%) and 12 days (4.1%), respectively, and in 2005, from 317 monitored days, were 29 days (9.1%), 270 days (85.2%) and 18 days (5.7%), respectively (SoER, 2004; 2005). Those data show that air quality in Jakarta is not good since the "moderate" and "unhealthy" days account for more than 90% of the total days; the level "moderate" means it can lead to serious health effect

1 Doctoral Student, Graduate School of Environment and Life Engineering, Toyohashi University of Technology, Japan.
2 Professor, Department of Ecological Engineering, Toyohashi University of Technology, Toyohashi, 441-8580 Japan.
3 Research Associate, Dept. of Ecological Engineering, Toyohashi University of Technology, Toyohashi, 441-8580 Japan.

for members of sensitive groups. Several investigations (JICA and Bapedal, 1997; Syahril et al., 2002; Syafruddin et al., 2002) have been done on the air pollution problem in Jakarta.

For efficient air pollution abatement it is essential to understand the fundamental mechanisms of air pollutant transport and transformation. These mechanisms are decisively influenced by the dynamics of the atmospheric boundary layer and local flow. In the last several decades much efforts have been devoted to clarify effect of local flows such as sea and land breezes on air pollutant transport (for example, Kitada, 1987, Kitada and Kitagawa, 1990; Lu and Turco, 1994; Simpson, 1994; Kunz and Moussiopoulos, 1995; Clappier et al. 2000; Grossi et al. 2000).

Jakarta has two distinct seasons of "dry" and "wet". The dry season continues from May to October and various local flows such as land and sea breezes develop every day. The intense sea breeze circulation tends to develop partly because the prevailing large scale winds of southeasterly and easterly in the dry season are blocked below an altitude of about 2 km by the high mountains extending along the southern coast of Java and the synoptic winds are weak in Jakarta (Sofyan et al., 2007).

To examine the effect of sea and land breezes on air pollution transport of NO_2 and SO_2 over Jakarta, meteorological and air pollution characteristics were investigated in the dry season, 6-17 August 2004. For the investigation, firstly, we made field measurements using a number of passive samplers of NO_2 and SO_2. Secondly, numerical simulations using PSU-NCAR MM5 for the analysis of meteorology, and air pollution transport simulations using a chemical transport model (CTM) described in Kitada et al. (1993, 2000) and Kitada and Regmi (2003).

In this paper, measured spatial distributions of NO_2 and SO_2 are compared with the numerical simulation for model validation; then various characteristics in NO_2 and SO_2 transports caused by the land/sea breezes in Jakarta are discussed.

2. Methodology and Data

2.1 Measurement of spatial distribution of NO_2 and SO_2

Spatial distributions of NO_2 and SO_2 over Jakarta city were measured by using passive samplers at 50 locations in August 2004; both one day (9 August; a weekday) and one week (10-17 August). The passive samplers were the products by Green Blue Co., Japan. We briefly summarize the results (see Sofyan et al. 2007 for detail).

Measurements were conducted at urban sites near main road, in main business area, populated housing area, and industrial complex, and also at several sub-urban sites surrounding Jakarta. One day averaged NO_2 and SO_2 concentrations showed overall maxima of 80.8 and 9.4 ppb and minima of 9.6 and 1.2 ppb, respectively (Fig. 3). One week averaged NO_2 and SO_2 concentrations were lower than one day averaged with overall maxima of 61.3 and 8.5 ppb and minima of 3.3 and 0.4 ppb, respectively. These observations suggest SO_2 concentrations in Jakarta are rather low.

2.2 Chemical Transport Model

Chemical Transport Model (CTM) was used to perform chemical transport calculation in Jakarta.

The CTM includes all of the important processes, such as advection, diffusion, gas, and aerosol phase chemistry, and dry and wet depositions. The model is an extension of that by Kitada et.al (1993) and Carmichael et al. (1986). The model includes 79 chemical species and a system of 163 chemical reactions. The CTM was used for air pollution transport studies in Central Japan (Kitada et al. 2000) and Kathmandu Valley, Nepal (Kitada and Regmi, 2003).

The horizontal domain covered 95 x 175 km^2 area (Fig. 1a) with variable grid sizes. The finest grid was used in central area (Jakarta city) such as 1 x 1 km grid for 40 x 40 km^2 area. The outer area surrounding Jakarta was covered by coarser grid sizes such as 1.5 km, 3 km, and 4.5 km; the coarsest grid size was used nearby domain boundary. The total number of horizontal grid points was 53 x 68. Vertical domain extends from the ground surface to a height of 10 km above mean sea level. The total number of vertical grids was 20 and these grid points were defined as terrain following variable grid size was used; for example, the grid heights over the sea surface are 2 m, 10 m, 40 m, 100 m, 200 m, 300 m, 500 m, 700 m, 1 km, 1.5 km, 2 km, 2.5 km, 3 km, 3.5 km, 4 km, 5 km, 6 km, 7 km, 8.5 km, and 10 km.

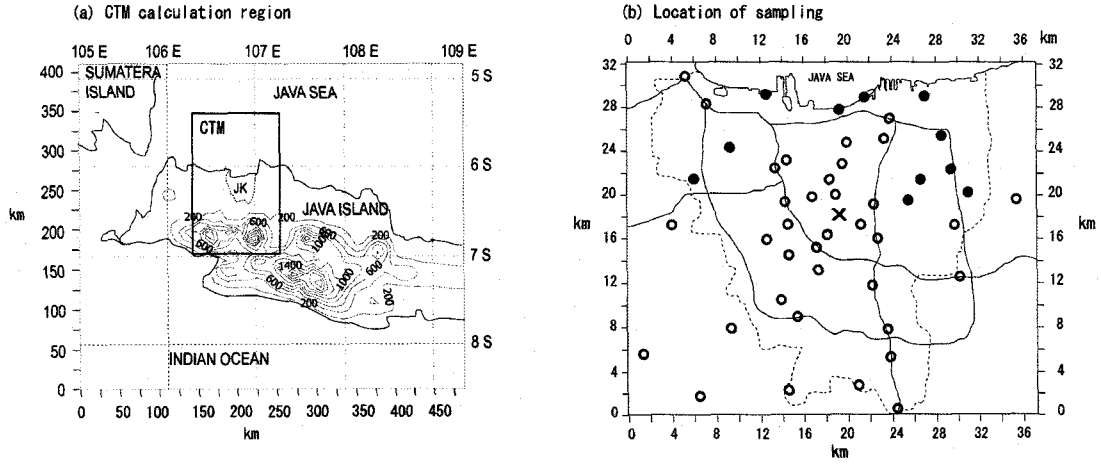

Figure 1. Calculation region for CTM simulation: the area enclosed with thick solid line, covered 94 km x 175 km wide area; there are Jakarta (is shown as JK) and the surrounding area, (b) Locations of sampling over Jakarta city; the solid circles, blank circles, and "X" show sampling points on industrial, business, and high building, respectively. The dashed line shows boundary of Jakarta city and the solid line shows main road network in Jakarta city.

2.3 Emission source data

The emission source distributions in 2004 for NO_X and SO_X were estimated based on the investigation for the 1995 emissions by JICA and Bapedal (1997); in this study, GDP growth factor of Jakarta from 1995 to 2004 was mainly used to extrapolate them to those in 2004. The estimated values were well compared with the emissions derived from total energy consumption in the sectors of transportation, industry, household (the energy consumption data from BPS, 2004). The estimation of the emission source is described elsewhere in detail (Sofyan et al., 2007). Table 1 summarizes the obtained NO_X and SO_X emissions in 2004.

Table 1. Estimated emission strength of NO_X and SO_X in the Greater Jakarta in 2004.

Sources by type	NO_X (as NO_2 in ton $year^{-1}$)	SO_X (as SO_2 in ton $year^{-1}$)
- Automobiles	139,788 (72.6%)	11,664 (16.9%)
- Factories	44,198 (22.9%)	51,236 (74.3%)
- Household/office	5,954 (3.1%)	5,064 (7.3%)
- Ships	2,626 (1.4%)	994 (1.4%)
Total	192,566 (100%)	68,958 (100%)
Sources by area	**NO_X (as NO_2 in ton day^{-1})**	**SO_X (as SO_2 in ton day^{-1})**
- Land (automobiles, factories, households/offices)	520.4 (98.6%)	186.2 (98.6%)
- Sea (ships)	7.2 (1.4%)	2.7 (1.4%)
Total	527.6 (100%)	192.0 (100%)

* The Greater Jakarta: the area including cities of Jakarta, Bogor, Depok, Tangerang, and Bekasi.

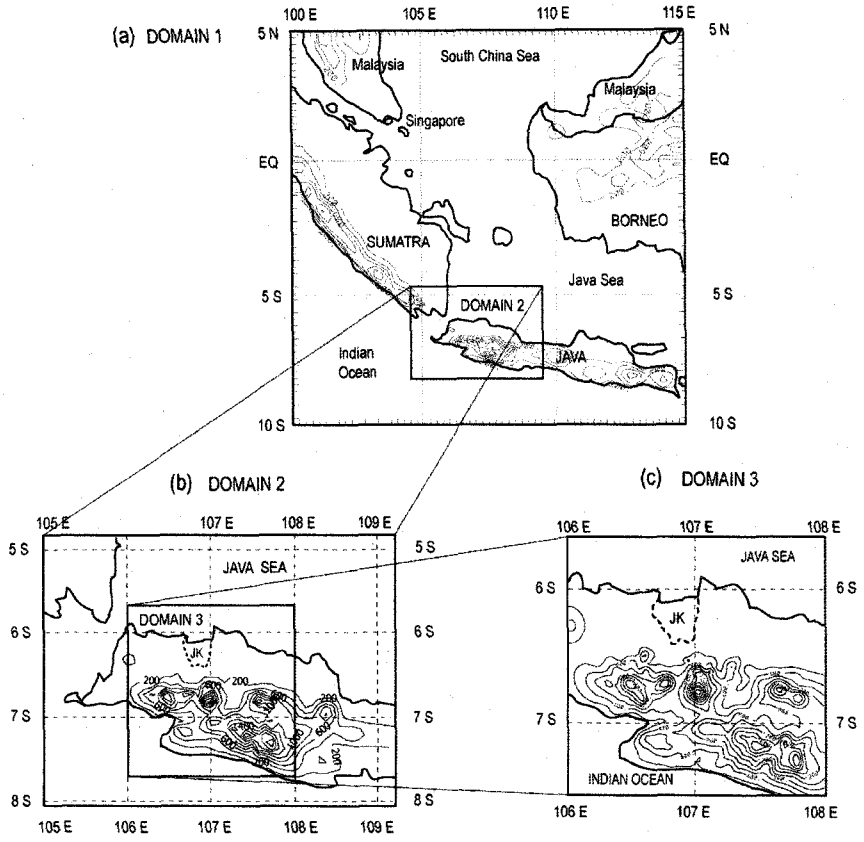

Figure 2. Domain system for MM5 simulation in Western Indonesia area: Domain 1 (a), 2 (b) and 3 (c).

2.4 Meteorology field data

Numerical simulation of wind flow on 6-17 August 2004 in the dry season has been performed using meso-scale PSU-NCAR MM5 (see Dudhia and Gill, 2005 for the detail of the software). The calculation was done by using 3 domains which use triply nested two-way interacting system (see Figure 2). Domain 1, 2, and 3 used 27, 9, and 3 km grid sizes, respectively. The physical processes applied in the simulations are Grell's subgrid scale cumulus convection, MRF's boundary layer parameterization, mixed-phase's cloud micro physics, and RRTM's long wave radiation. Each domain has 23 vertical grid points for the depth from the earth's surface to 100 hPa. The framework of meteorology in larger scale was provided every 6 hours by the operational archive of ECMWF with a resolution of 0.5° x 0.5°. In each calculation used was a land-use map with 25 categories and 30 second horizontal resolution by United States Geological Survey (USGS); the land use map was further modified by referring newly urbanized area in Jakarta.

Surface measurements from Geophysics and Meteorology Agency of Jakarta at Sukarno Hatta Airport (SH) were used to compare with the numerical calculation. As a result, the simulations have successfully reproduced meteorological observations at several weather stations in Jakarta and flow fields in the western Java (Sofyan et al., 2007).

Then the meteorological fields (e.g. three-dimensional winds, temperatures, humidity, eddy diffusivity, mixing ratio) and topographical characteristics (e.g. land use and surface roughness for individual land use categories) were used as input data for the CTM calculation.

3. Results and Discussion

3.1 Comparison of CTM simulations with field measurement

To examine the performance of the CTM simulation, the calculated concentrations of NO_2 and SO_2 were compared point for point with the observed values as can be seen in Fig. 3. Figure 4 shows excellent agreement between calculation and observation for NO_2 with a correlation coefficient, R=0.91 and acceptable agreement for SO_2 with R=0.76.

Figure 5a shows spatial distribution of observed NO_2 for 1-day-averaged (9 Aug. 2004) over Jakarta. As can be seen in Fig. 5b, the calculation well captures the observed NO_2 distribution. The high NO_2 zone is located near main roads, with the highest zone in the center of Jakarta city.

Spatial distributions of SO_2 are shown in Figs. 5c, d. The high SO_2 zone is located in specific industrial area nearby the city boundaries both in northern, western, eastern and southern Jakarta. Figure 5b indicates that the calculation quite well reproduced the characteristics of observed SO_2.

The vertical profiles of measured NO_2 (Fig. 6a) and SO_2 (Fig. 6b) are plotted. The measurements were carried out using passive samplers placed on the balconies and roof of a 110 m tall office building at the city center of Jakarta and about 10 km from the coastline. In Fig. 6, both measurement and calculations show that 1 day averaged NO_2 and SO_2 concentration are higher than 1 week averaged concentration. The CTM calculation again produced observed NO_2 profiles quite well (Fig. 6a) but rather failed to reproduce observed SO_2 profiles (Fig. 6b). The observed SO_2 profiles

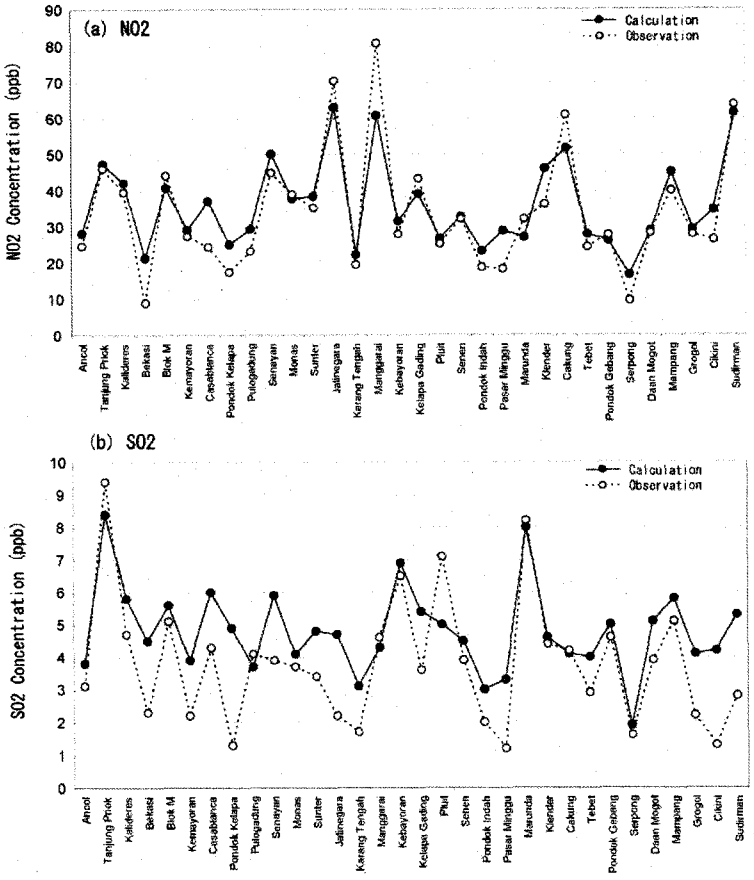

Figure 3. Site-by-site comparison between observations and CTM calculation for (a) NO_2 and (b) SO_2 daily average (9 Aug. 2004).

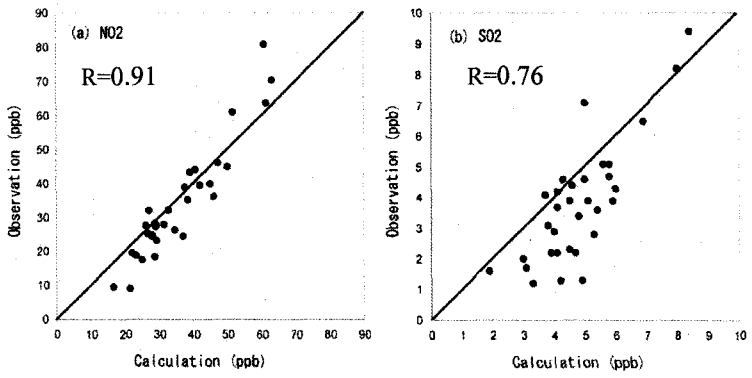

Figure 4. Scatterplots of one-day (9 Aug.2004) observation vs calculation for (a) NO_2 and (b) SO_2.

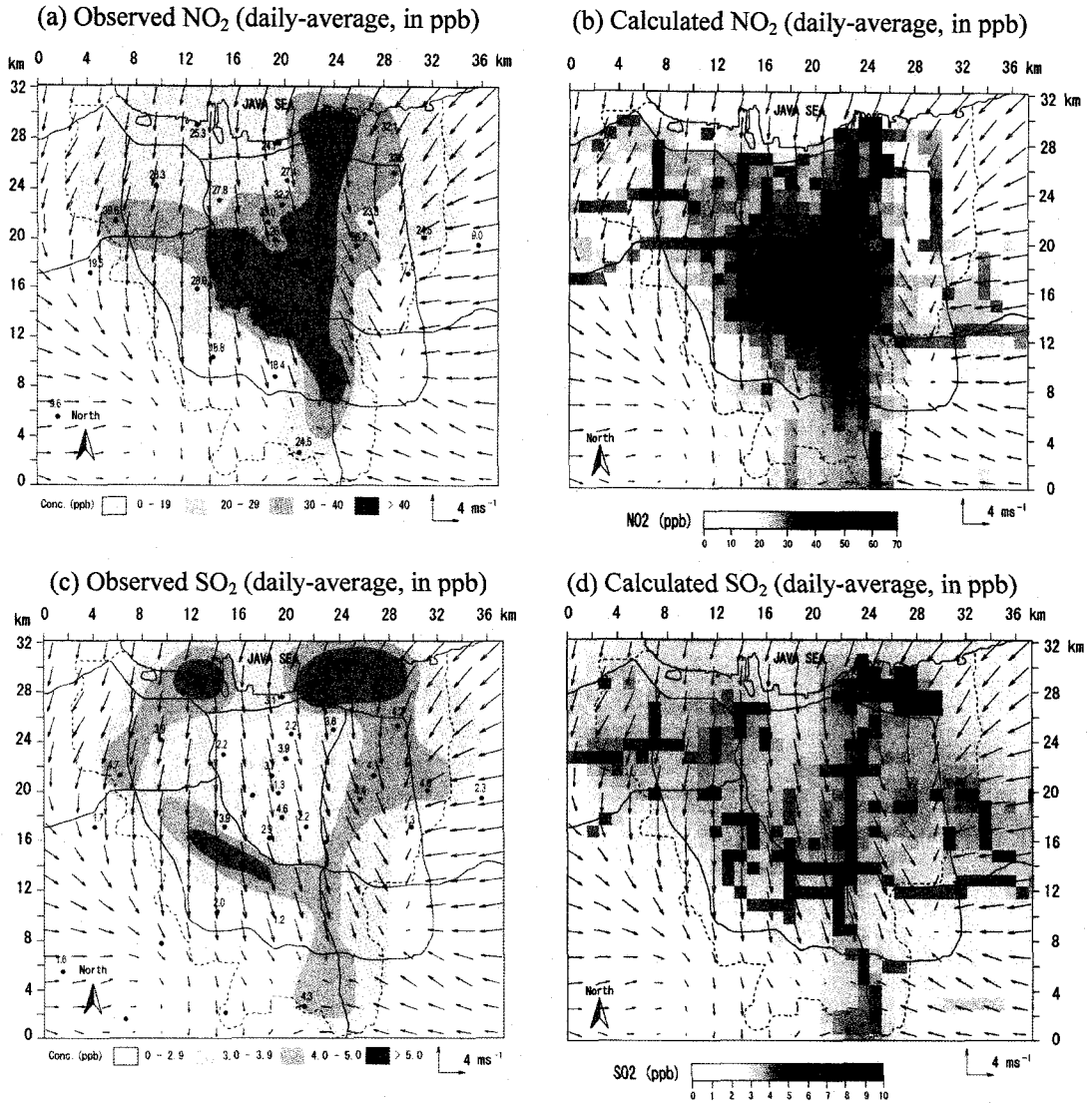

Figure 5. Horizontal distribution of 24-h-averaged concentration (ppb) over Jakarta city at 9 Aug. 2004, at surface level for (a) observed NO_2, (b) calculated NO_2, (c) observed SO_2, and (d) calculated SO_2. In Fig. 5a, c, the location of observation and observed concentration are shown by dot point and the values (ppb). The boundary of Jakarta city is shown by the dashed line (as can be seen as JK at Fig. 1a) and the main road network by solid line.

suggest higher SO_2 concentrations at 110 m, roof of the building. Since there are big power plants in the coastal Jakarta, this high SO_2 concentration may be due to the huge point sources of the power plants. Though the simulation has relatively large number of grid points in the boundary layer such as 2, 10, 40, 100, and 200 m, the horizontal grid size of 1 km in the simulation may not be enough to resolve the effect of the power plants.

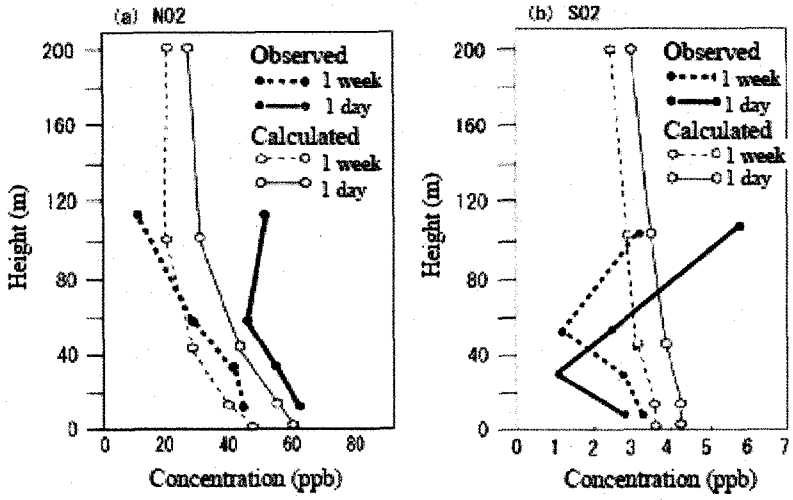

Figure 6. Comparison of vertical profiles of observed (thick line) and calculated (thin line) (a) NO_2 and (b) SO_2. Solid lines show daily average (9 Aug. 2004) and dashed lines show weekly average (10-17 Aug. 2004). Observation heights (black circles) were 15, 35, 55, and 110 m above ground.

3.2 Characteristics of NO_2 distribution

To show how flow fields affect pollutant distributions, both horizontal and vertical cross sections of the calculated flow and pollutants' concentrations are plotted in Figs. 7 and 8; Fig. 7 for the horizontal cross sections of NO_2, and Fig. 8 for the vertical cross sections. Figure 9 illustrates temporal changes of vertical profiles of calculated NO_2 at sites aligned north-south from the coast to the mountainous area: coastal (1 km inland), city center (15 km inland), southern Jakarta (35 km inland), and mountainous (55 km inland).

(1) Temporal development of NO_2 field

Figure 7a shows horizontal distribution of surface NO_2 at 0900 LST on 9 Aug. 2004. Around 0900 LST, wind in Jakarta is very weak because it is the time for alternation of the local flow system from land breeze to sea breeze under the characteristic weak synoptic scale wind condition. Note that the synoptic southeasterly can be seen over Java Sea off the coast and the southern mountains in Fig. 7a. In this situation, NO_2 in Fig. 7a shows localized high concentration zones due to surface emissions.

At 1200 LST (Fig. 7b) an early stage of sea breeze, that is northerly, develops in the coastal Jakarta, while "urban wind" blowing from the southern rural area toward the city center forms southerly. Hence, as illustrated in Fig. 8b, a convergence of the horizontal winds is generated over the central Jakarta. High NO_2 concentration zone roughly corresponds to this convergence line.

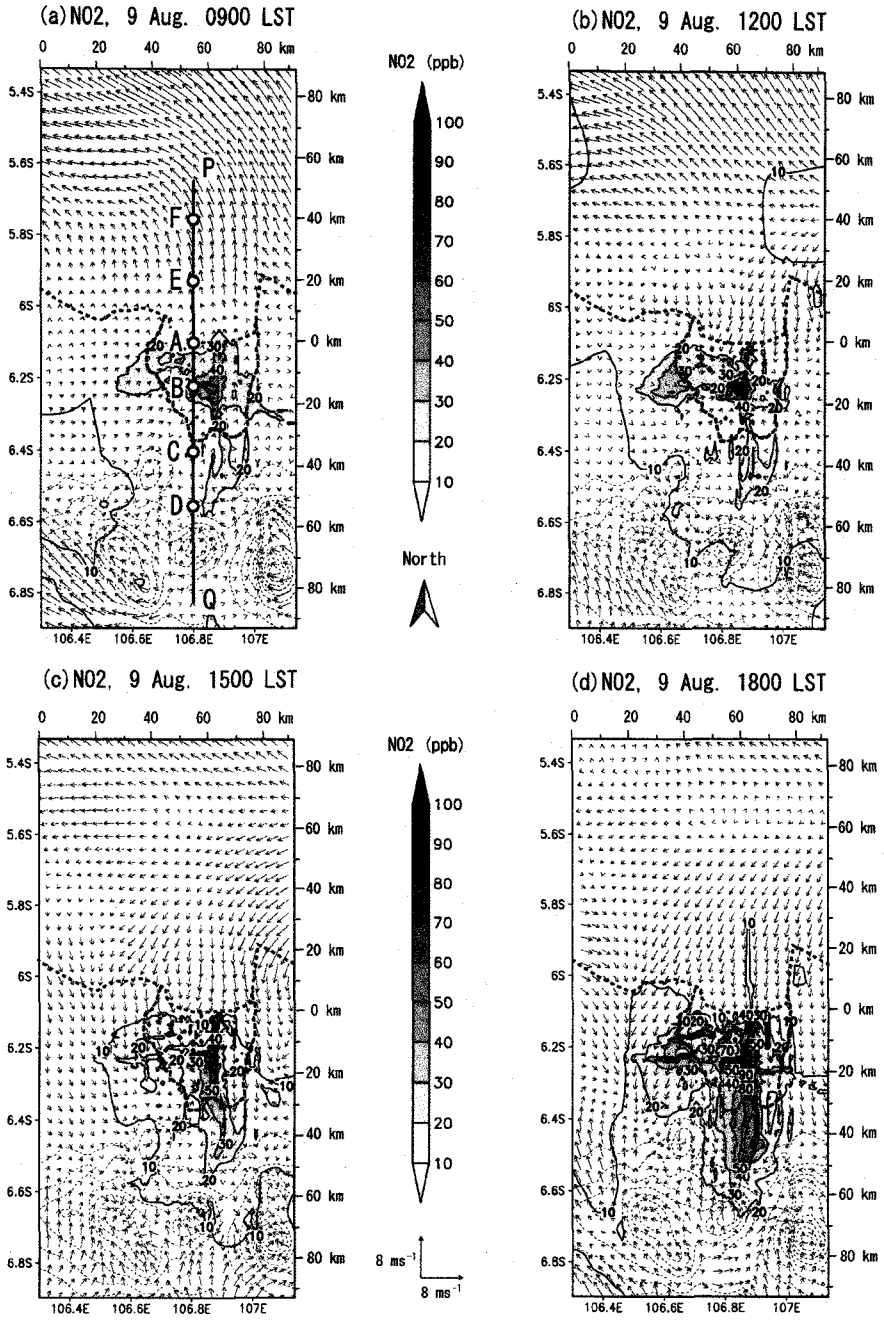

Figure 7. Diurnal variation of the horizontal field of calculated NO_2 (ppb) near the ground level: (a) 0900, (b) 1200, (c) 1500, (d) 1800, (e) 2100, (f) 2400 LST on 9 Aug., (g) 0300, and (h) 0600 LST on 10 Aug. 2004. The line PQ in Fig. 7a shows where vertical cross sections of NO_2 (Fig. 8) and SO_2 (Fig. 11) are drawn; the points A, B, C, and D represent "Coastal (1 km inland)", "City Center (15 km inland)", "Southern Jakarta (35 km inland)", and "Mountainous (55 km inland)", respectively; these are referred in Figs. 9 and 12.

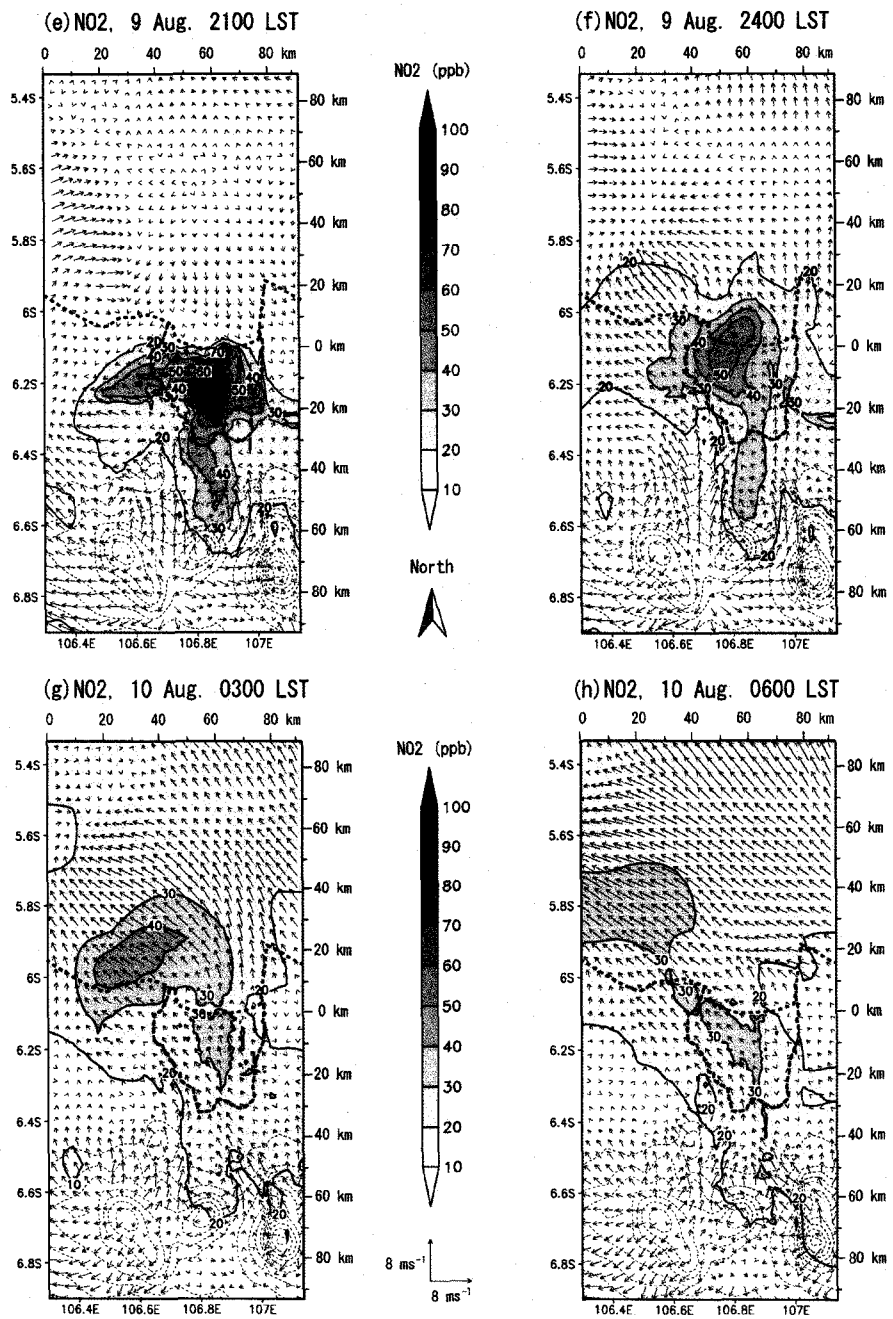

Figure 7. Continued

At 1500 LST (Figs. 7c and 8c) the "urban wind" is finally overcome by the sea breeze, and then the sea-breeze front further advances inland. Urban polluted air moves with the front as shown in Fig. 8c. Because of the synoptic flow adverse to the sea breeze, the sea breeze from Java Sea can reach

only at the hill of about 60 km from the coast at 1800 LST (see Fig. 8d). During these hours, the pollutants are transported with the sea breeze further inland (Figs. 7d and 8d), and lead to higher NO_2 concentrations over southern Jakarta and mountainous area. By 1900 LST the sea-breeze circulation gradually decays and ceases around 2000 LST.

At 2100 LST almost no wind blows at surface level in Jakarta (Fig. 7e), and stably stratified surface layer, formed by the weak local wind and radiational cooling of the ground surface after sunset, accumulates primary pollutants such as NO_X and SO_2 over Jakarta. By 2400 LST land breeze and mountain wind start (see Figs. 7f and 8f), and thus by the local winds the pollutants accumulated in Jakarta are transported northward off the coast. The land breeze continues until morning.

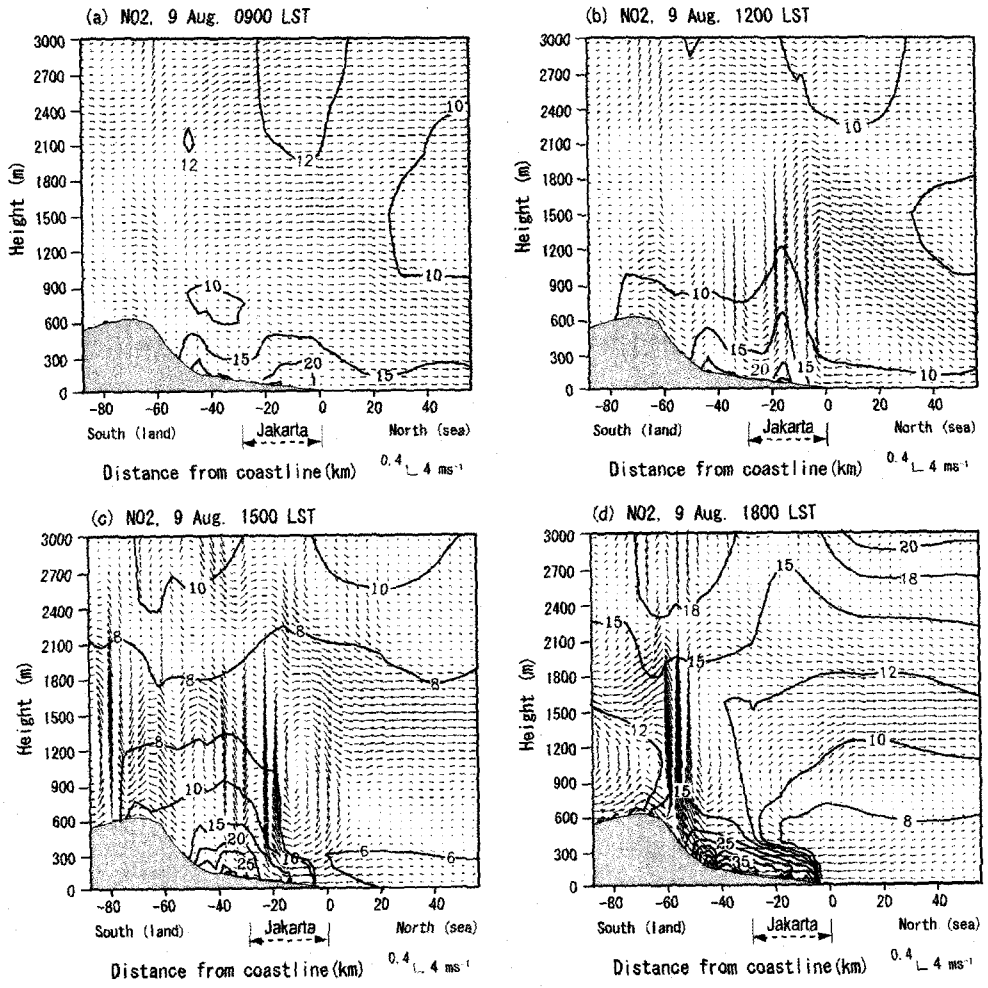

Figure 8. Diurnal change of the vertical cross section of calculated NO_2 (ppb) along line A-B (see Fig. 1b for the line A-B) is shown at: (a) 0900, (b) 1200, (c) 1500, (d) 1800, (e) 2100, (f) 2400LST on 9 Aug., (g) 0300, and (h) 0600 LST on10 Aug. in 2004. Contours are in ppb.

After 2400LST the land breeze and mountain wind transport NO_X rich air mass accumulated in Jakarta to Java Sea; hence they contribute to reduce NO_2 concentration in Jakarta (see Figs. 7g, h and 8g, h). Figures 7f,g,h indicates such a large volume of urban air mass with high NO_2 concentration is not formed again after 2400LST. The land breeze and mountain wind cease between 0600 and 0700LST, leaving again the region in weak surface wind condition before the next day's sea breeze will start. Diurnal changes shown in Figs. 7, 8 are repeated almost everyday in the dry season.

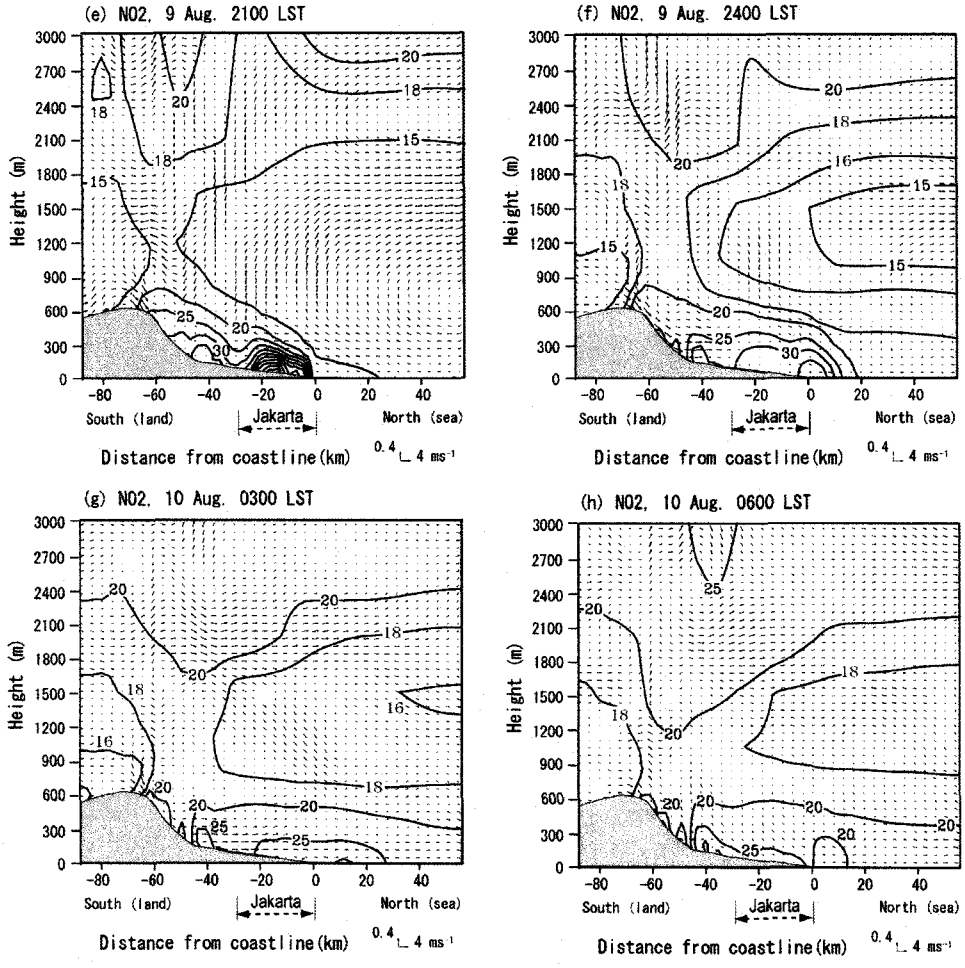

Figure 8. Continued.

(2) Vertical profiles of NO_2 at selected locations: area influenced by sea and land breezes

Figures 7 and 8 demonstrate the pattern of the NO_2 concentration field is largely affected by the local flows such as land/sea breezes and mountain/valley winds. In this sub-section, how these local flows modify vertical structure of NO_2 concentration will be examined in detail at various locations

from the coastal to mountainous areas. From Fig. 9a, at the coast ("A" in Fig. 7a) NO_2 concentration (and other primary pollutants) is relatively low under sea breeze situation and high at about 2400LST just before the land breeze carries away the pollutant toward the sea. Temporal variation of the NO_2 profile in Fig. 9b at the "city center" ("B" in Fig. 7a) is similar to that at the coast (Fig. 9a), but the NO_2 at 2100LST in the stably stratified and weak wind condition (see Fig. 7e) is much higher than that in Fig. 9a, because there are large emission sources around the "city center" site. Both Figs. 9a,b indicate depth of the polluted layer moving with the sea/land breezes is about 300 to 400 m.

At the "southern Jakarta" (the location "C" in Fig. 7a), the sea breeze arrives at 1500LST, and then NO_2 concentration starts to increase (see Fig. 9c), indicating that the NO_2 rich air mass reaches there with the sea breeze. Similarly, to the "mountain" site ("D" in Fig.7a), the sea breeze brings in additional NO_2 at 1800LST (see Fig. 9d). However the air mass, originated from Java Sea, can not further penetrate to the south because of the mountain wind developing after sunset and the synoptic scale flow which are adverse to the sea breeze (Figs. 7d,e and 8d,e). In short, the pollutant discharged in Jakarta area can be transported, by the sea breeze/valley wind, to about 60km from the Jakarta coast line (see Fig. 7 for distance from the coast line) at the foot of the southern mountains.

Next, we will see how far pollutants rich air mass can go with land breeze off the coast. Figures 9e and f show the vertical profiles of NO_2 at 20 and 40 km off the Jakarta coast on the same line P-Q shown in Fig. 7a, respectively. Figure 9f suggests NO_2 rich air mass starts to reach at 40 km off the coast at 0300LST, and the same air mass with its depth below 400m seems to have already covered the area at 20 km from the coast (Fig. 9e). Though it is not shown in this paper, the vertical profile of NO_2 at 60 km off the coast indicates the place is nearly end of the land breeze's influence. Thus we concluded the pollutants from Jakarta can be transported nearly 40 – 60 km from the coast line by the land breeze.

(3) NO_2 levels in Jakarta estimated by the calculation

Figure 7 suggests some area likely exceeds the National Ambient Air Quality Standard (NAAQS) of Indonesia in a typical sea/land breezes day in dry season; the standard is 150 $\mu g/m^3$ ($\approx$75 ppb) for one-day-averaged NO_2. For example, high emission area in central Jakarta shows severe air pollution especially during 1700-2100 LST.

3.3 Characteristics of SO_2 distributions

Diurnal variation of horizontal field of the calculated SO_2 is shown in Fig. 10. Similarly, a north-south vertical cross section of SO_2 along the line PQ in Fig. 7a is also plotted in Fig. 11. Finally, Fig. 12 presents temporal change of the vertical profile of SO_2 at selected locations along the line PQ in Fig. 7a.

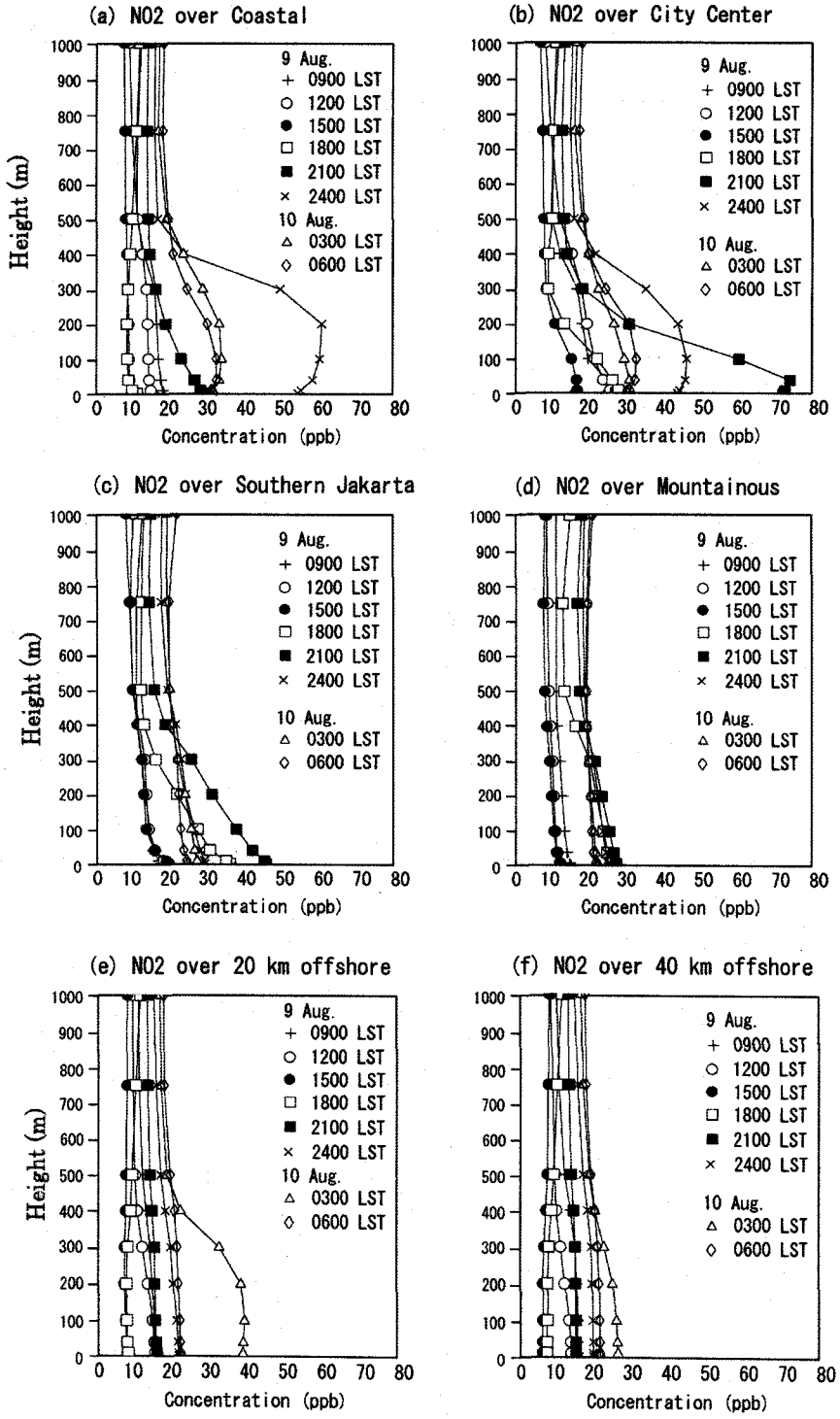

Figure 9. Diurnal variations of the vertical profile of NO_2 at the specific locations along the line PQ in Fig. 7a (a) coastal (1 km inland), (b) city center (15 km inland), (c) Southern Jakarta (35 km inland), (d) Mountainous (55 km inland), (e) 20 km, and (f) 40 km off the Jakarta shoreline.

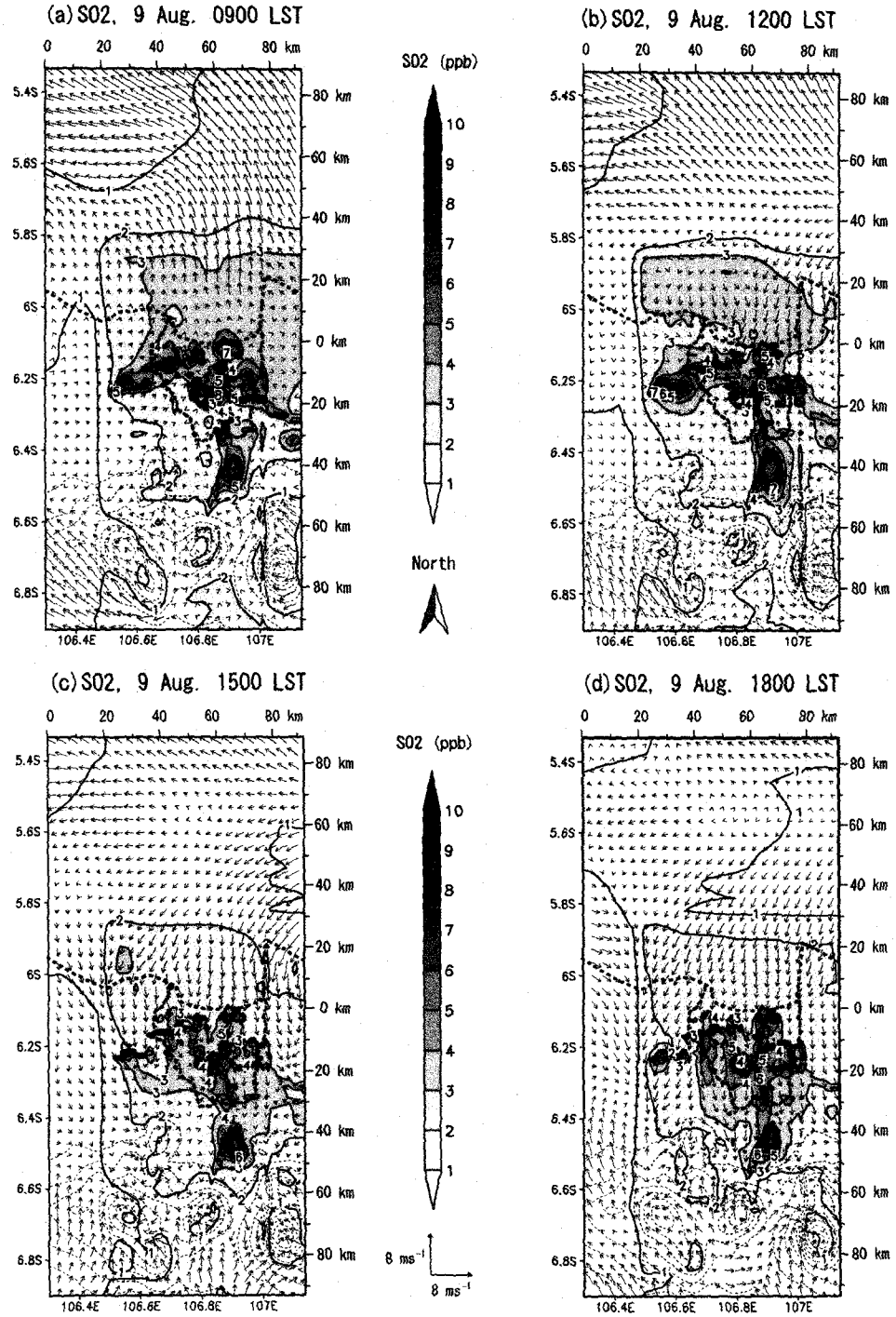

Figure 10. Same as Fig. 7 but for SO_2 (ppb).

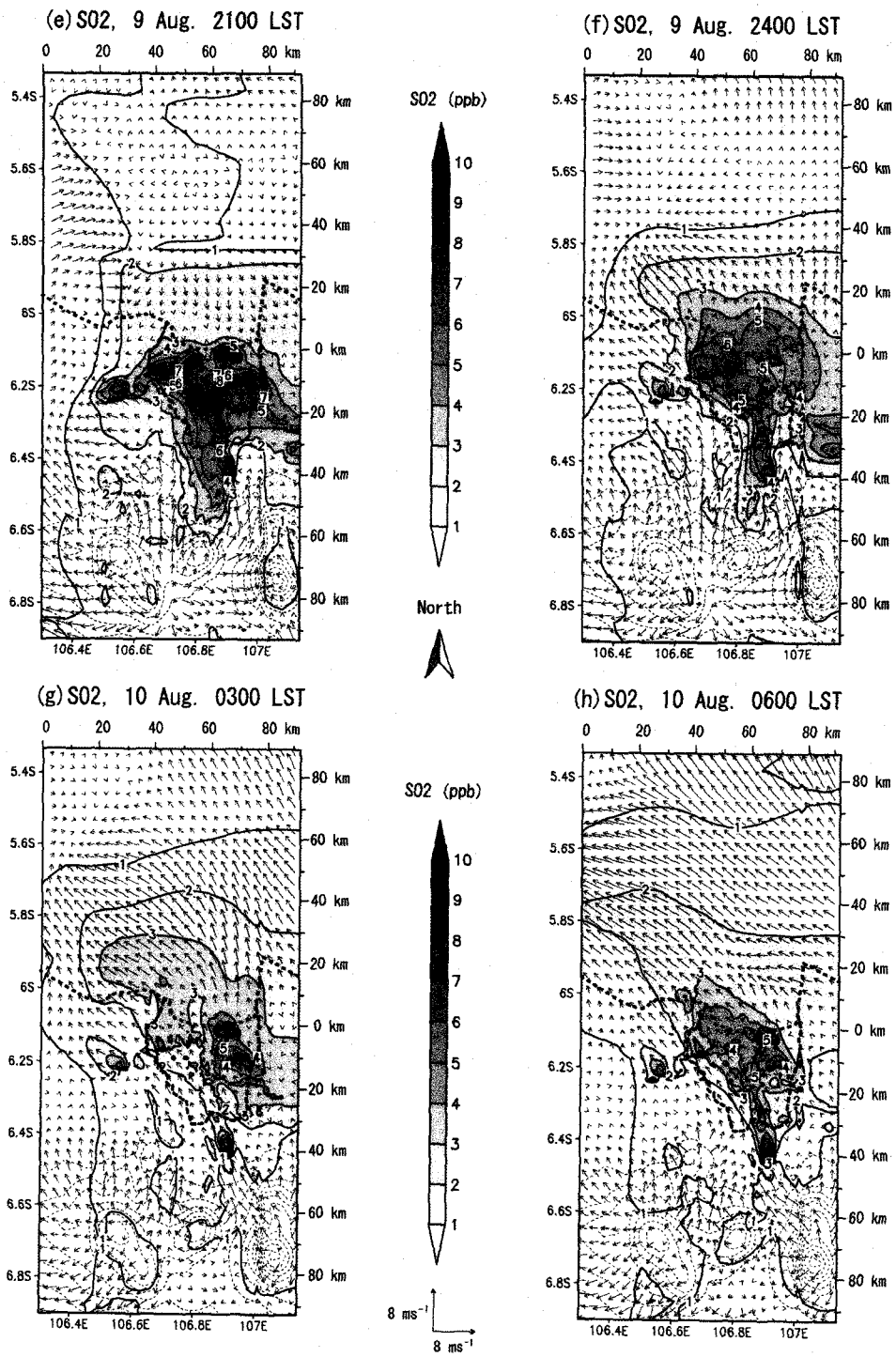

Figure 10. Continued.

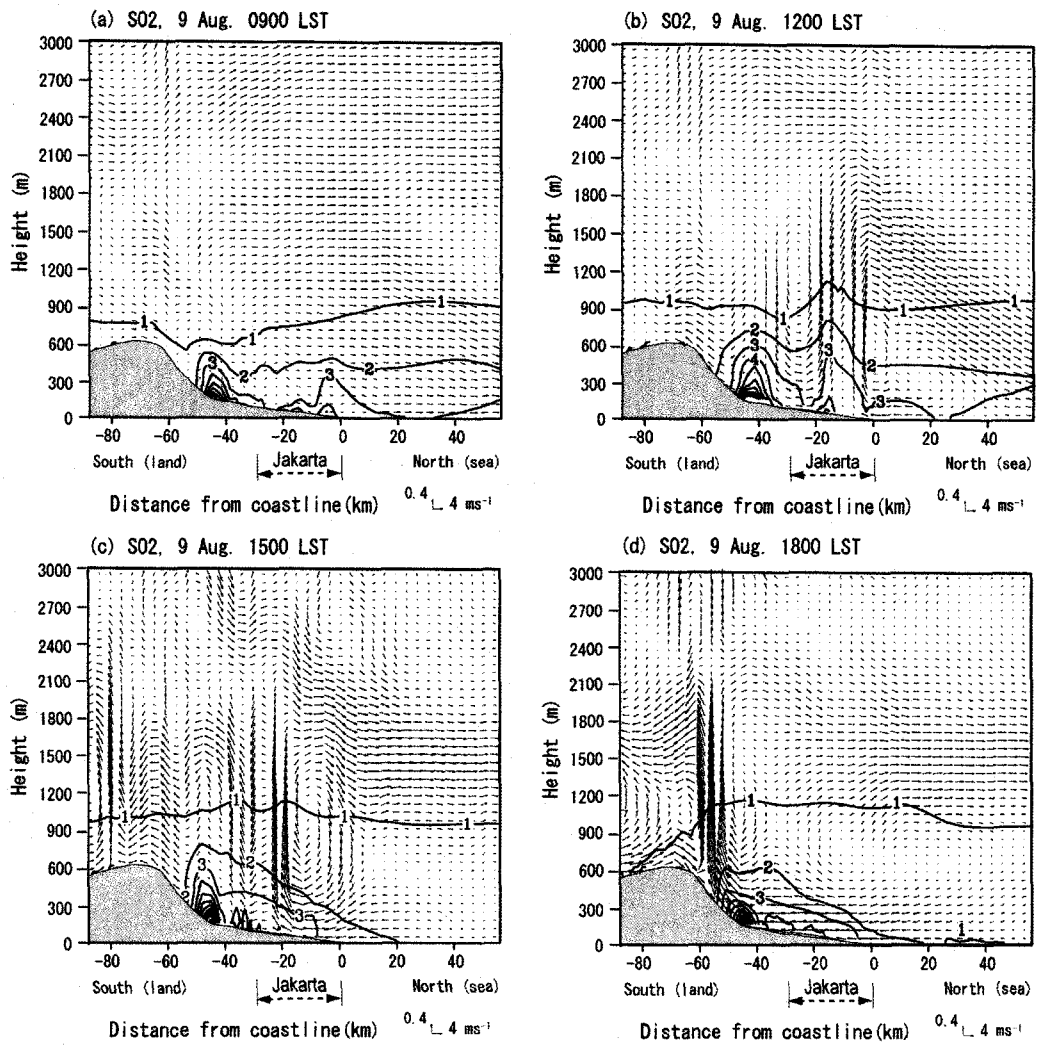

Figure 11. Same as Fig. 8 but for SO_2 (ppb).

(1) Characteristics in spatial distributions of SO_2 concentration: findings from CTM simulation

SO_2 distribution is nearly same as that of NO_2. But some differences can be observed because of the differences in the source distribution and chemical reactivity between SO_2 and NO_2; that is, (1) car emission accounts for about 70 % of the total NOx emission and, in particular, that from main roads in central Jakarta largely contributes it, while about 70 % of total SOx emission is from industrial complexes nearby north, east, south, and west borders of Jakarta, and a large part of this industrial SOx emission comes from tall stacks as point sources; (2) chemical reactivity of SO_2 is much smaller than that of NO_2, and thus SO_2 can be regarded as an inert tracer for the urban air mass originated from Jakarta.

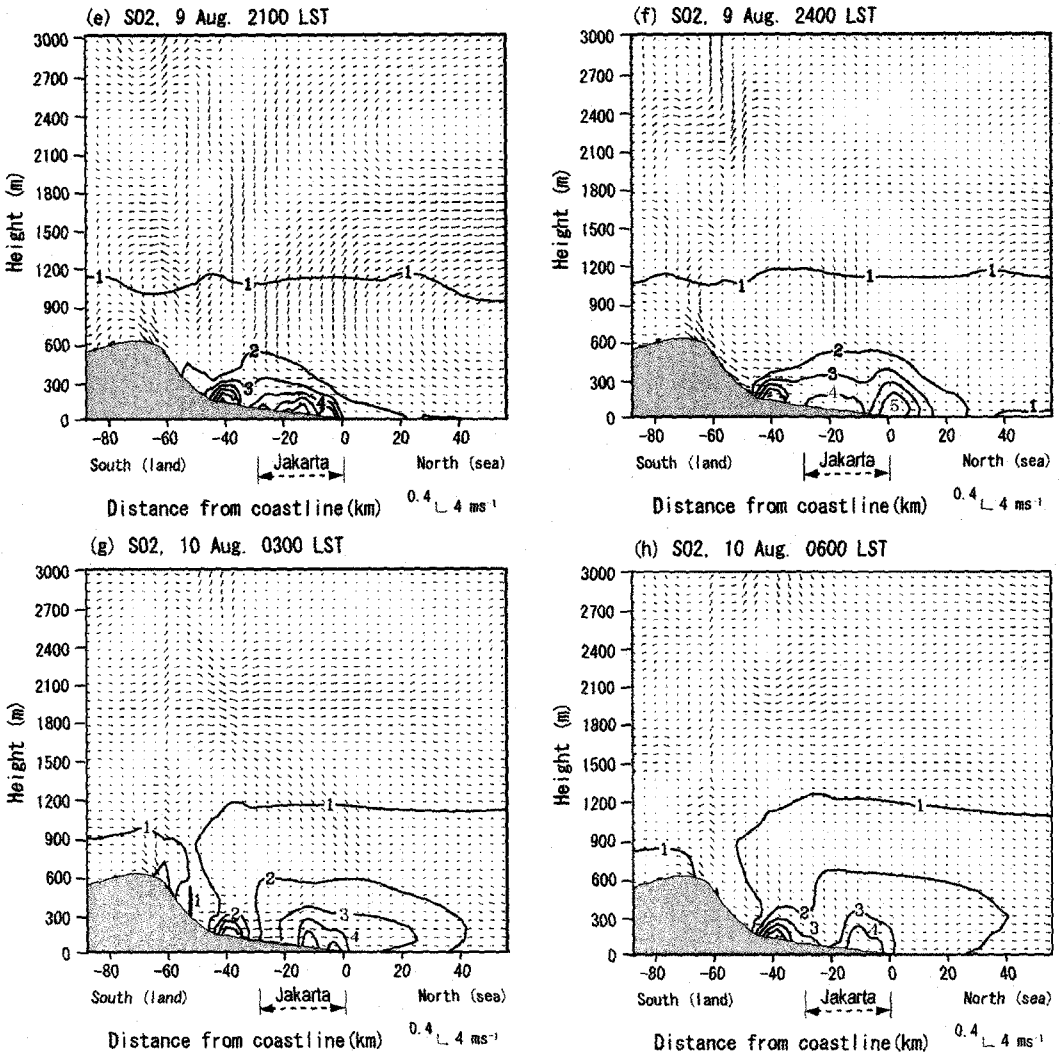

Figure 11. Continued

Figure 10a shows horizontal distribution of SO_2 near surface at 9:00LST on 9 Aug. 2004. Since the surface wind is very weak in Jakarta at the time of alternation of the local flow system from "land breeze" to "sea breeze", high SO_2 concentrations appear over the emission areas of industrial complexes and heavy traffic in central Jakarta. Over Java Sea 30 km off the coast, the land breeze enhanced by the synoptic southeasterly still transports the SO_2 rich polluted air mass further northward.

By 1200 LST (Fig. 10b) sea breeze develops in the coastal area. Though the SO_2 horizontal distribution (Fig. 10b) is qualitatively same as NO_2 (Fig. 7b), SO_2 in Fig. 10b more clearly shows the urban air mass once moved over Java Sea again comes back to the Jakarta coast. After this onset of

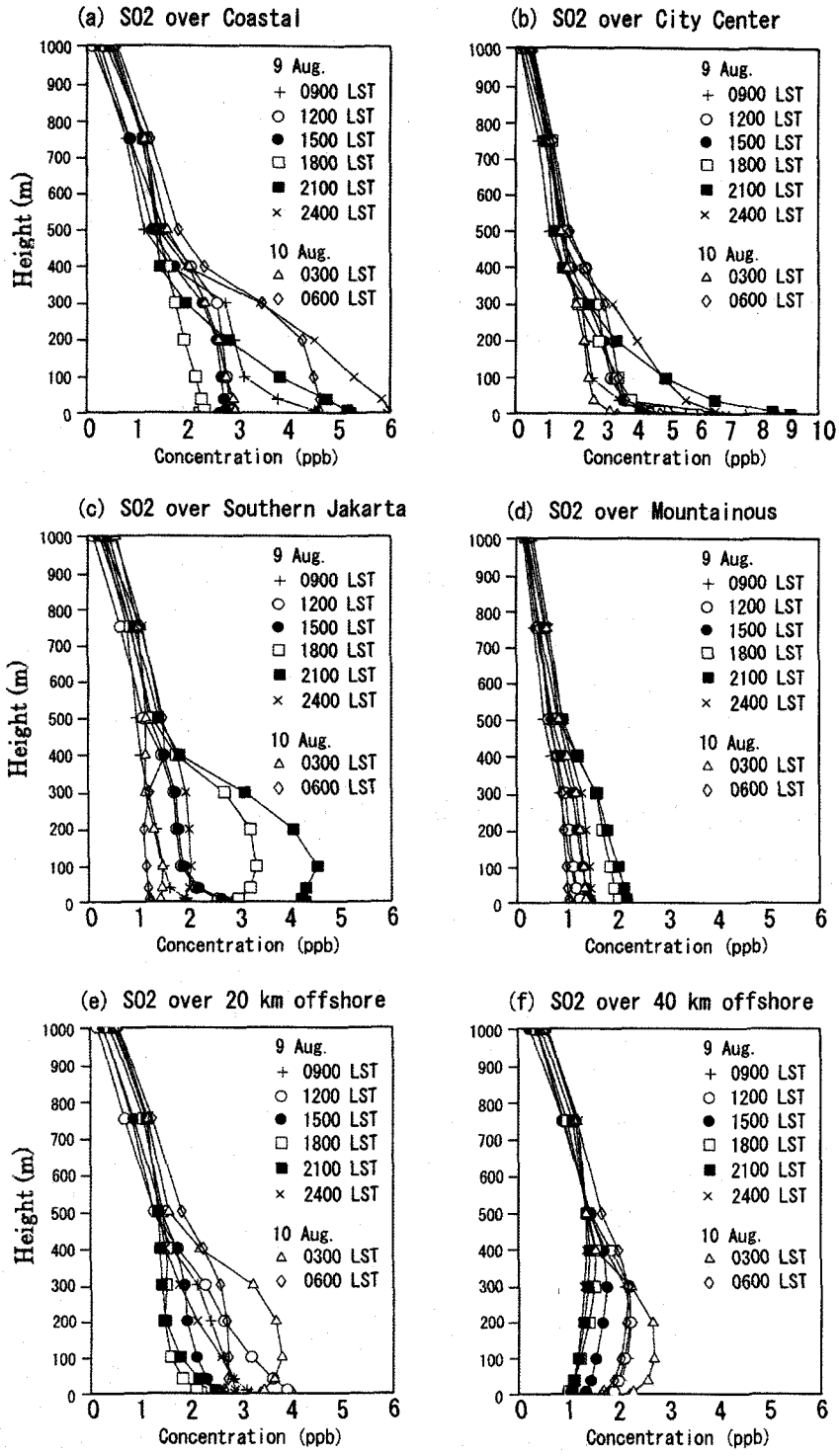

Figure 12. Same as Fig. 9 but for SO_2 (ppb).

the sea breeze, the relatively less- SO_2 marine air decreases SO_2 concentration in the coastal area as shown in the temporal change of SO_2 in Fig. 12a. At 1500 LST (Fig. 10c) the sea-breeze front reaches at the southern edge of Jakarta about 25 – 30 km from the coast (see Fig. 11c) by overcoming an urban wind (see wind at 20 km from the coast in Fig. 11b) blowing into the heated city center from the south. Because of the strong industrial emission at 40 km inland, the SO_2 concentration is always high there (see Figs. 10 and 11), which is very different from the NO_2 distributions in Figs. 7 and 8.

At 1800 LST (Fig. 10d) the sea breeze front reaches most inland at about 60 km from the coast line. During the nighttime, mountain wind starts at 2100 LST (see Figs. 10e and 11e) and after 2400LST land breeze also joins in the mountain wind (Figs. 10f and 11f), and the polluted urban air mass of Jakarta is again carried toward Java Sea (Figs. 10g,h and 11g,h).

(2) Characteristics of vertical mass transport associated with local flow systems: findings from vertical profiles of the calculated SO_2

Vertical profiles of SO_2 (Fig. 12) at various locations on the line PQ in Fig. 7a demonstrate how each location is affected by the dynamics of land/sea breeze and mountain/valley wind. One interesting thing is that at all locations transfer of SO_2 to upper layer over a height of 400 m is very small, indicating SO_2 discharged over Jakarta remains below 400 m, which is also depth of the sea breeze, and mainly moves horizontally.

After 2400 LST (Fig. 12f) under land breeze circulation, SO_2-rich air mass migrates toward Java Sea, decreases SO_2 concentration in city center, southern and mountainous areas (Fig. 12b, c, d), and in turn, increases SO_2 in the coastal area (Fig. 12a). The land breeze continues until 0700 LST.

3.4 Effects of sea/land breezes and mountain/valley winds on dynamics of air pollutant's mass budget

Effects of sea/land breezes and mountain/valley winds on the dynamics of air pollutant's mass budget were investigated for the area of 94 km (east-west) x 174 km (north-south); the area has the same length of 87 km for both land and sea sides in the north-south direction, and entirely covers the Greater Jakarta on the land side. For vertical direction, a depth of 500 m was taken for lower and upper layers; that is, the lower layer is assumed to extend from the earth's surface to 500 m high, while the first upper layer is from 500 to 1000m above the ground and the second upper layer is from 1000 to 1500 m. To know mass budget of air pollutants is important firstly because we can know how much percent of primary pollutants discharged in an area can be removed in the same area by processes such as dry deposition and thus how much percent of the pollutants can be long transported into the free troposphere, and secondly because role of the local flows such as sea/land breezes and mountain/valley winds in the pollutant transport from a near-surface layer to upper layer can be quantitatively evaluated. It may be noted that photochemical production of O_3 and its dynamics were simultaneously calculated for 6-17 Aug 2004, showing O_3 is produced over Java Sea in the afternoon, intrudes into Jakarta and the southern mountainous area with sea breeze, and can remain over Jakarta even in land breeze in the early morning though its concentration level is low (Kitada et al., 2008).

(1) Dynamics of the mass of SO_x in the layer below 1.5 km under land- and sea-breezes in dry season

Purpose of this subsection is to examine how the mass of SO_2, a major primary pollutant, behaves under sea/land breeze circulations in the stable tropical weather of dry season in Western Java. Figure 13a and b show three-day variations, 8-10 Aug. 2004, of the SO_2 and SO_4^{2-} mass in the six boxes of L1-L3 and S1-S3 (see Fig. 13a), respectively. Figure 13a and b suggest several interesting things:

(a) Mass in box S1 over Java Sea is about 0.5 to 1.0 times as much as that in box L1 which is over emission area. This result that the amount of SO_2 in box S1 is yet comparable to that in L1 indicates "land breeze" combined with mountain wind is strong enough to result in large mass transport from land area to Java Sea during the nighttime and in the early morning.

(b) In the first upper layer (from 500m to 1000m above the surface), the amount of SO_2 in box L2 ranges from 45% to 80% of that in box L1 while over Java Sea the SO_2 mass in box S2 is about 50 to 100% of that in S1, indicating quite large amount of SO_2 is lifted from the boxes, L1 and S1, in the lower layer to L2 and S2. Flow mechanisms contributing these mass transports can be thought as a mixed layer activity developed over the land area prior to penetration of the sea breeze and vertical motion at the sea breeze front enhanced by a southerly urban wind blowing toward Jakarta. Since the depth of the sea breeze layer is relatively shallow, at most 500m, in Jakarta and is capped by a stable layer, no significant upward mass transport is expected in the area already covered with the sea breeze layer.

(c) To estimate pollutant transport from boundary layer to free troposphere such as upper layer above a height of 1 km is interesting to know subsequent possible impact of anthropogenic emissions from tropical area on regional and global scale pollution. From Fig. 13a, the amount of SO_2 in the upper layer above 1 km high can be estimated as about 8-10% of those below 1 km; the percentage was obtained by dividing mass in both boxes of L3 and S3 by the sum of those in L1, L2, S1, and S2.

(d) Diurnal variation of the mass in L1 and S1 apparently reflect diurnal nature of land- and sea-breezes as well as emission activity.

(d.1) On the SO_2 mass in L1, for example, from 2400 to about 0700LST box L1 looses the mass to box S1 because of developed land breeze. Then the SO_2 mass in L1 again starts to and continues to increase till about noon in a calm condition due to cease of the land breeze and no sea breeze developed in the coastal area and enhanced emission activity in the morning. After 1200LST till 1800LST SO_2 mass in L1 again decreases probably because of three reasons; one is that the advancing sea breeze front transports the mass in L1 to the upper box L2 and additionally to the box L3 (see Fig. 13a), the second reason is that SO_2 is oxidized to SO_4^{2-} in photochemical reactions as seen in Fig. 13b showing diurnal variations of the SO_4^{2-} mass, and the third reason may be the dry deposition process enhanced in the turbulent thermal internal boundary layer. The diurnal pattern described here is typical for L1, and is repeated everyday (see "L1" in Fig. 13a).

(d.2) Temporal variation of the SO_2 mass in S1 over Java Sea is mainly characterized by the alternation of land and sea breezes; a typical example is shown on 10 Aug. in Fig. 13a. For example, during the nighttime from 2100LST on 9 Aug to around 1000LST on 10 Aug, the mass in S1 continues to increase due to the land breeze, and it decreases after 1100LST till 1800LST on 10 Aug because sea breeze brings SO_2 over Java Sea out to land area.

(e) Patterns of diurnal variations of SO_4^{2-} in L1 and S1 (Fig. 13b) are simpler than those of SO_2 and show only one peak in the afternoon; this is because SO_4^{2-} is produced mainly by a chemical reaction with OH radical which is potentially high in the photochemical smog reactions during the daytime; the aqueous phase oxidation of SO_2 is not assumed in this dry season study.
(f) A notable feature found in both SO_2 and SO_4^{2-} in Figs. 13a and b is these pollutants' accumulation, suggesting that the land and sea breeze circulations, repeated under stable synoptic weather condition, trap these pollutants within them; this accumulation may be dissolved by occasional enhancement of the synoptic scale easterly and southeasterly.

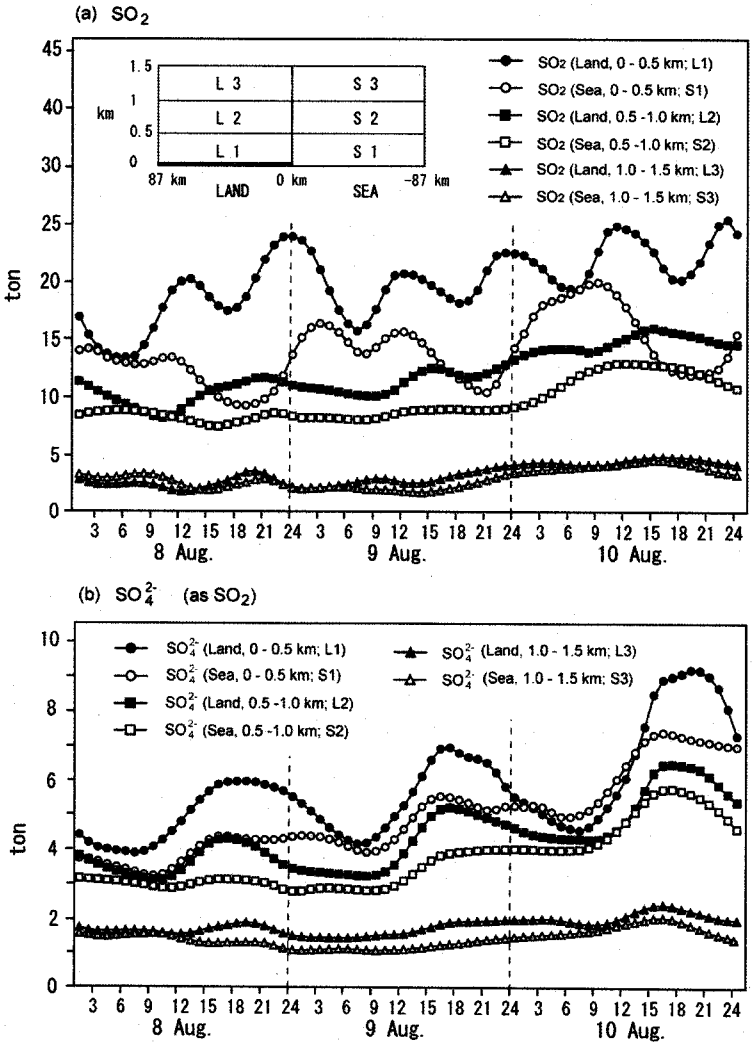

Figure 13. Diurnal variations of the mass of (a) SO_2 and (b) SO_4^{2-} in boxes L1 ~ L3 and S1 ~ S3 during 8-10 Aug. 2004.

(4) Dynamics of the mass of N compounds in the layer below 1.5 km under land- and sea-breezes in dry season

In the previous sub-section we have discussed in detail dynamics of SOx in three layered boxes with a thickness of 500m each over land and sea surfaces (see Fig. 13a). Here we examine dynamics of the mass of NOx (NO and NO_2) as primary pollutants and other N-containing products such as HNO_3, PAN (Per-oxy Acetyl Nitrate), and N_2O_5 in boxes with 1000 m thick and 87 km long over land and sea surfaces. Figure 14 shows diurnal variations of (a) NO, NO_2 and HNO_3, and (b) PAN and N_2O_5 in the boxes of LL1 (land) and SS1 (sea). From Figs. 14a and b, we can observe the followings:
(a) On temporal change of each N-containing compound, its same pattern is repeated for three days, indicating again influence of repeated same types of local flows in sunny condition under stable synoptic weather.

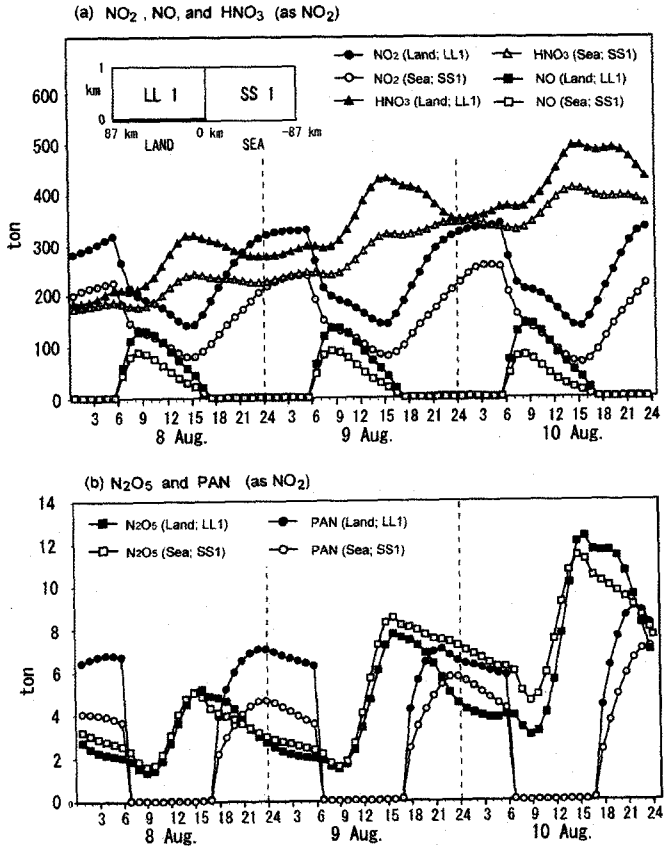

Figure 14. Diurnal variations of the mass of (a) NO_2 , NO and HNO_3, and (b) N_2O_5 and PAN in box LL1 and SS1 during 8-10 Aug. 2004.

(b) On primary and quasi primary compounds, NO and NO_2, NO has emission sources and is discharged always to some extent, but during the nighttime the emitted NO is rapidly oxidized to NO_2 by the reaction with ambient O_3 without any reverse mechanism from NO_2 to NO. Hence NO mass becomes very small after sunset while NO_2 increases. In the daytime, since the photolysis reaction of NO_2 always reproduces NO, NO has its largest value together with its high emission activity.
(c) HNO_3 and PAN are products of photochemical smog reactions. That is, HNO_3 is produced via NO_2 + OH reaction and secondarily heterogeneous process involving H_2O and N_2O_5 where N_2O_5 is formed by NO_2 + NO_3 and here NO_3 is mainly produced by NO_2 + O_3; meanwhile, PAN is the product of CH_3CO_3 + NO_2 reaction. However, there is some difference between temporal changes of PAN and HNO_3. As shown with open and solid circles in Fig. 14(b), PAN decreases in the daytime because of its strong thermal decomposition, and is again formed by the above recombination in the cooler condition after sunset. On the other hand, HNO_3 does not have significant loss mechanism except for dry deposition during the day- and night-time and conversion to particulates mainly during

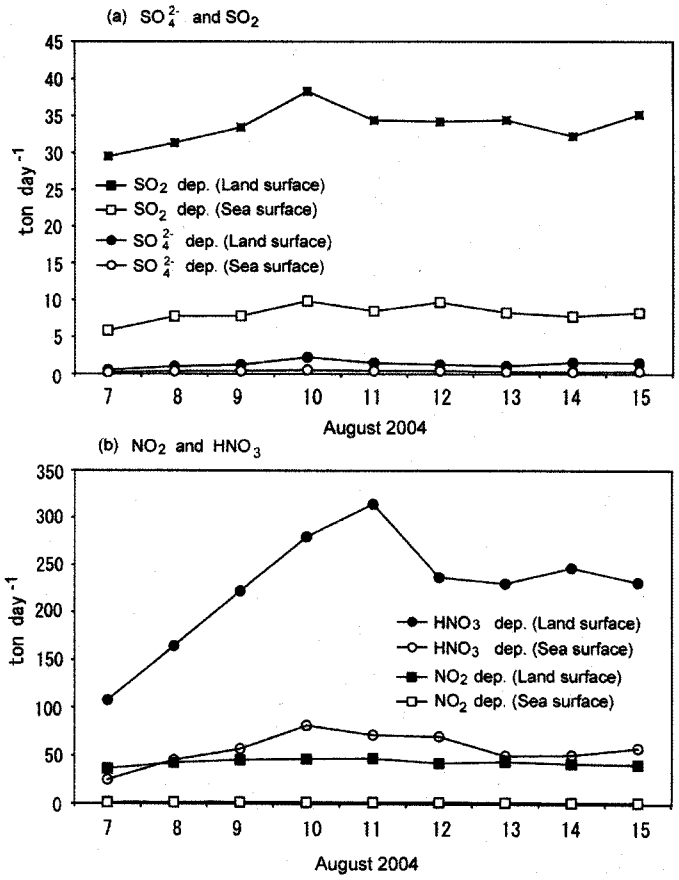

Figure 15. Temporal variation of dry-deposited mass of (a) SO_2 and SO_4^{2-} and (b) NO_2 and HNO_3 during 7-16 Aug. 2004. Unit is in ton-SO_2-equivalent/day for S-compounds (a) and ton-NO_2-equivalent/day for N-compounds (b). The area for dry deposition is the nearly same size for land and sea as shown, for example, in Fig. 7.

the nighttime; hence HNO_3 concentration shows rather monotonic increase with aenhanced increasing rate in the afternoon (see triangles in Fig. 14(a)). Figure 14 also indicates that among the products, production of HNO_3 is by far larger than the other species.

Table 2. Dry deposited mass of N- and S-compounds over land area including the Greater Jakarta and Java Sea (see Fig. 7) for the one day averaged over 7-15 August 2004. Percentage shows the ratio to the NOx and SOx emissions in the Greater Jakarta for one day.

		Ton/day	Percentage (ratio to NOx or SOx emission per day in the Greater Jakarta)
NO_2 dep.	Land	43.0	8.0 %
	Sea	1.5	0.3 %
HNO_3 dep.	Land	226.0*	42.0 %
	Sea	56.6*	10.5 %
	Total	327.1*	60.8 %
SO_2 dep.	Land	33.7	17.5 %
	Sea	8.2	4.3 %
SO_4^{2-} dep.	Land	1.4#	0.7 %
	Sea	0.4#	0.2 %
	Total	43.7#	22.7 %

* Ton-NO_2 equivalent/day. # Ton-SO_2 equivalent/day.

(d) Effect of land and sea breezes on the transport of N-compounds seems to be same as that on S-compounds. Accumulation of the products in the local flow circulations can be inferred also for N-compounds.

3.5 Dry deposition of S- and N-containing compounds: temporal variation and deposited total mass

Removal of N- and S-compounds due to dry deposition was evaluated. In the dry season dry deposition should be principal removal mechanism of the pollutants because of little wet deposition expected. Figure 15 shows nine-day variation of dry-deposited mass of (a) SO_2 and SO_4^{2-} and (b) NO_2 and HNO_3 over land and sea areas. Depending on dry deposition velocity and concentration of each pollutant, the dry deposited mass varies as shown in Fig. 15; that is, S-compounds is removed mainly as SO_2 and not as SO_4^{2-}. The reason can be thought as a much smaller deposition velocity (as

sub-micron particle) and lower concentration of SO_4^{2-} than SO_2. In contrast to S-compounds, N-compounds is largely removed as HNO_3 (major reaction product from NOx), reflecting that HNO_3 has a very fast dry deposition velocity and is produced quite rapidly in photochemical smog reactions.

Table 2 is a summary of calculated dry deposition and suggests that:

(a) Under local flow situation in the dry season, about 61% of NOx discharged by fuel combustion can be removed by dry deposition of mainly HNO_3 and additionally NO_2 over land and sea area in the calculation region (for example, see Fig. 7 for the region).

(b) Similarly, anthropogenic SOx emitted in the Greater Jakarta can be removed from the atmosphere by about 23% by dry deposition of mainly SO_2 and additionally SO_4^{2-}.

(c) The difference between NOx and SOx will be due to faster production of HNO_3 than SO_4^{2-} in the photochemical smog reactions and much larger dry deposition velocity of HNO_3 than that of SO_4^{2-}.

4. Summary and Conclusions

By using a chemical transport model (CTM), which is a comprehensive model including processes of transport, chemistry and deposition for air pollutants, together with the meso-scale meteorological model MM5, air pollution characteristics over Jakarta were numerically investigated in the dry season during 6-17 August, 2004. The followings were found in this study:

1) The CTM model was shown to produce fairly accurate results of the NO_2 and SO_2 concentration distribution when compared with available observations with a correlation coefficient for NO_2 and SO_2 of R=0.91 and R=0.76, respectively.

2) Jakarta is characterized by weak synoptic scale wind below 1 km high since the large scale prevailing winds (easterly and south-easterly) are blocked by the high southern mountains. Thus the sea- and land-breeze circulations are repeated everyday in Jakarta area. The simulations demonstrated that the sea and land breezes largely characterize the air pollution over Jakarta area; the diurnal cycle of the concentrations of NO_2 and SO_2 are influenced by the sea breeze.

3) In the morning before 1100LST, under calm condition after cease of land breeze and before onset of sea breeze in coastal Jakarta, NO_2 and SO_2 concentrations become high in the emission source area. These high concentrations in the coastal Jakarta are eased by the relatively clean marine air reached with sea breeze in the early afternoon. At noon the depth of the sea breeze layer is about 400-500 m, and its front is located at about 15 km inland.

4) By 1500 LST the sea-breeze front reaches about 30 km inland, and the whole Jakarta city is covered by the sea breeze layer. By 1800 LST, the sea breeze merges with the up-slope wind, and finally the marine air reaches at the hill of about 60 km from the coast. Thus the pollutants transported with the sea breeze slightly raise those concentrations over southern Jakarta and mountainous area. Then, the sea breeze gradually reduced its wind speed. By 1900 LST the sea-breeze circulations gradually start to decay and cease around 2000 LST.

5) By 2100 LST the sea breeze stopped and almost no wind blows in Jakarta; the region is dominated by weak surface wind and the concentrations increase. Hence, in general, nighttime

concentration of NO_2 and SO_2 over Jakarta is higher than daytime. In the case of NO_2 oxidation of NO by O_3 also largely contributes to its higher concentration.

6) By 2400 LST land breeze starts and the pollutants are transported with the land breeze, lowering the concentrations over center and southern Jakarta while over coastal area the concentrations increase. The land breeze continues until morning.
7) An interesting feature of the sea breeze in Jakarta in the dry season is that the sea breeze layer remains always shallow at about 400 ~ 500 m, and this causes that pollutants released into the sea breeze layer over Jakarta and the other emission areas do not disperse vertically, remain in the shallow layer, and rather move back and forth with the sea and land breezes, leading to accumulation of the pollutants in the shallow local flows. The upward motion associated with sea breeze front activity seems only mechanism which lifts pollutants in lower layer to the height above 1 km.
8) Because of the suppressed vertical transport of the pollutants, dry deposition of the pollutants onto the earth's surface seems effective process for their removal; as shown in Table 2, it was estimated that about 60% of NOx and 23% of SOx discharged in one day over the greater Jakarta are removed from the atmosphere within the same day.

Acknowledgements

This work was supported in part by Grant-in-Aid for Scientific Research (B), No. 17360256 by Ministry of Education, Culture, Sports, Science, and Technology, Japan, and Global Environment Research Fund, No. C-051 (Project leader: Dr. Shiro Hatakeyama) by Ministry of the Environment, Japan. We are grateful to the JSPS-MOE Core University Program on Urban Environment for its support to this study. Asep Sofyan appreciates support by Grant-in-Aid for the 21st century COE Program: "Ecological Eng. for Homeostatic Human Activities", the Hori Information Science Promotion Foundation, and the Fuji Xerox Setsutaro Kobayashi Memorial Fund, Japan.

References

BPS (2004): *Jakarta in Figures 2004*, BPS-Statistics of DKI Jakarta Province, 524 pp.

Carmichael, G.R., Peters, L.K., and Kitada, T. (1986): A second generation model for regional-scale transport/chemistry/deposition, *Atmospheric Environment,* Vol. 20, 173-188.

Clappier, A., Martilli, A., Grossi, P., Thunis, P., Pasi, F., Krueger, B.C., Calpini, B., Graziani, G., Bergh, H.V.D. (2000), *Journal of Applied Meteorology*, Vol. 39, 546-562.

Dudhia, J. and Gill, D. (2005): *PSU/NCAR Mesoscale Modeling System Tutorial Class Notes and User's Guide: MM5 Modeling System Version 3,* Mesoscale and Microscale Meteorology Division, National Center for Atmospheric Research.

Grossi, P, Thunis, P., Martilli, A., Clappier, A. (2000) : Effect of Sea Breeze on Air Pollution in the Grater Athens Area. Part II: Analysis of Different Emission Scenarios, *Journal of Applied Meteorology*, Vol. 39, 563-575.

JICA and Bapedal (1997): *The study on the integrated air quality management for Jakarta metropolitan area: Final Report,* Volume I, Main Report, 10 Chapters.

Kitada T. (1987): Turbulence structure of sea-breeze front and its implication in air pollution

transport – application of turbulence model - , *Boundary Layer Meteorology*, **41**, 217-239.

Kitada, T, Sofyan, A. and Kurata, G. (2008): Numerical simulation of air pollution transport under sea/land breeze situation in Jakarta, Indonesia in dry season, *Air Pollution Modeling and Its Application XIX,* Elsevier, in press.

Kitada, T. and Kitagawa, E. (1990): Numerical analysis of the role of sea-breeze fronts on air quality in coastal and inland polluted areas, *Atmospheric Environment*, Vol. 24A, 1545-1559.

Kitada, T., Lee, P.C.S, Ueda, H. (1993): Numerical Modeling of long-range transport of acidic species in association with meso-β-convective clouds across the Japan Sea resulting in acid snow over coastal Japan. I. Model description and qualitative verifications. *Atmospheric Environment,* Vol. 27A, 1061-1076.

Kitada, T., Okamura, K., Nakanishi, H., and Mori, H. (2000): Production and Transport of Ozone in Local Flows over Central Japan – Comparison of Numerical Calculation with Airborne Observation – , *Air Pollution Modeling and Its Application XIII*, Kluwer Academic/Plenum Publishers, 95-106.

Kitada, T. and Regmi, R. P. (2003): Dynamics of air pollution transport in late wintertime over Kathmandu Valley, Nepal: As revealed with numerical simulation, *Journal of Applied Meteorology*, Vol 42, 1770-1798.

Kunz, R. and Moussiopoulos, N. (1995): Simulation of the Wind Field in Athens using Refined Boundary Conditions, *Atmospheric Environment*, Vol. 29, No. 24, 3575-3591.

Lu, R. and Turco, R.P. (1994): Air Pollutant Transport in a Coastal Environment. Part I: Two-Dimensional Simulations of Sea-Breeze and Mountain Effects, *Journal of the Atmospheric Sciences,* Vol. 15, No. 15, 2285-2308.

Simpson, J. E. (1994): *Sea-breeze and Local Wind*, Cambridge University Press, 234 p.

Sofyan, A., Kitada, T, and Kurata, G. (2007): Difference of Sea Breeze in Jakarta between Dry and Wet Seasons: Implication in NO2 and SO2 Distributions in Jakarta, *Journal of Global Environment Engineering,* Vol. 12, 63-85.

SoER (2004): *State of Environment Report of Indonesia 2004*, Ministry of Environment, Indonesia, 256 p.

SoER (2005): *State of Environment Report of Indonesia 2005*, Ministry of Environment, Indonesia, 283 p.

Syahril, S., Resosudarmo, B.P., Tomo, H.S. (2002) *Study on Air Quality in Jakarta, Indonesia*, ADB Report, 82p.

Syafruddin, A., Budiman, B.T., Resosudarmo, B.P., Harwati, F., Tomo, H.S., Loedin, L., Soejachmoen, M.H., Restiti, N.G.A., Tamin, R.D., Manurung, R., Syahril, S., and Rosenthal., S. (2002) *Integrated Vehicle Emission Reduction Strategy for Greater Jakarta, Indonesia,* ADB Report, 80p.